# Sustained reduction of essential tremor with low-power non-thermal transcranial focused ultrasound stimulations in humans

Thomas Bancel, Benoît Béranger, Maxime Daniel, Mélanie Didier, Mathieu Santin, Itay Rachmilevitch, Yeruham Shapira, Mickael Tanter, Eric Bardinet, Sara Fernandez Vidal, et al.

Brain Stimulation 17 (2024) 636–647

Contents lists available at ScienceDirect

Brain Stimulation

journal homepage: www.journals.elsevier.com/brain-stimulation

# Sustained reduction of essential tremor with low-power non-thermal transcranial focused ultrasound stimulations in humans☆

Thomas Bancel [a], Benoît Béranger [b], Maxime Daniel [a], Mélanie Didier [b], Mathieu Santin [b], Itay Rachmilevitch [c], Yeruham Shapira [c], Mickael Tanter [a], Eric Bardinet [b], Sara Fernandez Vidal [b], David Attali [a,d], Cécile Galléa [b], Alexandre Dizeux [a], Marie Vidailhet [b,f], Stéphane Lehéricy [b,e], David Grabli [f], Nadya Pyatigorskaya [b,e], Carine Karachi [g], Elodie Hainque [f], Jean-François Aubry [a,*]

[a] Physics for Medicine Paris, Inserm U1273, ESPCI Paris, CNRS UMR 8063, PSL University, Paris, France
[b] ICM-Paris Brain Institute, Centre de NeuroImagerie de Recherche-CENIR, Inserm U 1127, CNRS UMR 7225, Sorbonne Université, F-75013, Paris, France
[c] Insightec, Tirat Carmel, Israel
[d] Université Paris Cité, GHU-Paris Psychiatrie et Neurosciences, Hôpital Sainte Anne, F-75014, Paris, France
[e] Department of Neuroradiology, Hôpital de la Pitié Salpêtrière, Sorbonne Université, AP-HP, Paris, France
[f] Department of Neurology, Hôpital de la Pitié Salpêtrière, Sorbonne Université, AP-HP, Paris, France
[g] Department of Neurosurgery, Hôpital de la Pitié Salpêtrière, Sorbonne Université, AP-HP, Paris, France

ARTICLE INFO

*Keywords:*
Transcranial ultrasound stimulation
Essential tremor
Skull aberration correction
MR-Guidance
Accelerometry

ABSTRACT

*Background:* Transcranial ultrasound stimulation (TUS) is a non-invasive brain stimulation technique; when skull aberrations are compensated for, this technique allows, with millimetric accuracy, circumvention of the invasive surgical procedure associated with deep brain stimulation (DBS) and the limited spatial specificity of transcranial magnetic stimulation.
*Objective:* /hypothesis: We hypothesize that MR-guided low-power TUS can induce a sustained decrease of tremor power in patients suffering from medically refractive essential tremor.
*Methods:* The dominant hand only was targeted, and two anatomical sites were sonicated in this exploratory study: the ventral intermediate nucleus of the thalamus (VIM) and the dentato-rubro-thalamic tract (DRT). Patients (N = 9) were equipped with MR-compatible accelerometers attached to their hands to monitor their tremor in real-time during TUS.
*Results:* VIM neurostimulations followed by a low-duty cycle (5 %) DRT stimulation induced a substantial decrease in the tremor power in four patients, with a minimum of 89.9 % reduction when compared with the baseline power a few minutes after the DRT stimulation. The only patient stimulated in the VIM only and with a low duty cycle (5 %) also experienced a sustained reduction of the tremor (up to 93.4 %). Four patients (N = 4) did not respond. The temperature at target was 37.2 ± 1.4 °C compared to 36.8 ± 1.4 °C for a 3 cm away control point.
*Conclusions:* MR-guided low power TUS can induce a substantial and sustained decrease of tremor power. Follow-up studies need to be conducted to reproduce the effect and better to understand the variability of the response amongst patients. MR thermometry during neurostimulations showed no significant thermal rise, supporting a mechanical effect.

☆ Parts of the results have been presented at:- 23rd international symposium on therapeutic ultrasound, Lyon, France, April 2023 (First in man deep brain ultrasound stimulation for Essential Tremor)- 4th Focused Ultrasound Neuromodulation Conference, Stanford, California, July 2023 (Exploring the Feasibility of Deep Brain Ultrasound Stimulation for Essential Tremor: Results from a First-in-Human Study).

* Corresponding author. 2-10 rue d'Oradour-sur-Glane, 75015, Paris, France.
*E-mail address:* jean-francois.aubry@espci.fr (J.-F. Aubry).

https://doi.org/10.1016/j.brs.2024.05.003
Received 12 December 2023; Received in revised form 3 May 2024; Accepted 3 May 2024
Available online 9 May 2024

**Abbreviations**

| | |
|---|---|
| TUS | transcranial ultrasound stimulation |
| VIM | ventral intermediate nucleus |
| DRT | dentato-rubro-thalamic |
| MR | magnetic resonance |
| DBS | deep brain stimulation |
| TMS | transcranial magnetic stimulation |
| ET | essential tremor |
| OCD | obsessive-compulsive disorders |
| VEP | visually evoked potential |
| fMRI | functional magnetic resonance imaging |
| CRST | clinical rating scale for tremor |
| MP2RAGE | magnetization prepared 2 rapid acquisition gradient echoes |
| DTI-FT | diffusion tensor imaging fiber tracking |
| AC | anterior commissure |
| PC | posterior commissure |
| WS | workstation |
| FE | front-end |
| PRF | pulse repetition frequency |
| $I_{sppa}$ | spatial-peak pulse average intensity |
| MRgFUS | magnetic resonance-guided focused ultrasound |
| SEP | sensory evoked potentials |
| ACC | anterior cingulate cortex |
| MEP | motor evoked potentials |

## 1. Introduction

Essential tremor (ET) is one of the most prevalent neurological diseases [1]. It is characterized by bilateral upper-limb action tremor for at least 3 years [2]. For essential tremor that is refractory to pharmacotherapy, neurosurgical treatments are proposed [3], such as deep-brain stimulation (DBS) [4] and ablative therapy [5].

DBS is the gold standard physical treatment for the treatment of various movement disorders such as Parkinson disease [6], essential tremor (ET) [4,7] and dystonia [8]. In Essential tremor, the ventral intermediate nucleus of the thalamus (VIM) is the main target used for chronic neuromodulation in DBS [9]. Some authors have also proposed the direct neuromodulation of VIM afferences coming from the cerebellum and the dentato-rubro-thalamic tract (DRT) [10].

Transcranial Magnetic Stimulation (TMS) is a non-invasive neuromodulation technology [11] that has been used to achieve cerebellocortical inhibition [12] or pre-supplementary motor area stimulation [13,14] for essential tremor. Nevertheless, the wavelength of the TMS pulses is larger than the dimension of the human head, which precludes direct targeting of deep-seated targets like the VIM and the DRT [15].

Transcranial ultrasound stimulation (TUS) [16] holds promise for neurosurgical treatment of movement disorders such as ET. Ultrasound is non-invasive [17,18] and has millimetric accuracy [19,20] when administered with aberration correcting devices such as multi-element arrays [21,22] or acoustic lenses [19], giving it the potential to probe the therapeutic neurosurgical target used for DBS or lesional therapy.

Ultrasonic neuromodulation was first reported in the 50's by Fry et al. in cats [23] and confirmed by other groups in mice [24–30], rats [31–37][], lagomorphs [38], sheep [39], porcine [40], non-human primates [41–46] and humans [47–50]. Although the mechanism of action of TUS remains incompletely understood, several hypotheses have been proposed [16], including intra-membrane cavitation [51] and radiation force induced activation of mechano-sensitive ion channels [52]. Different ultrasound parameters have been reported to induce inhibition [27,53] or activation [38,54]. Biophysical models have been proposed to describe the underlying interaction of ultrasound with the neural network, with a vast majority of models highlighting the impact of mechanical effects [55–58], even though thermally-induced inhibition with low intensity focused ultrasound was reported recently [59]. Analogy can be made with DBS, where simulation of external electric fields produced by DBS were used to assess excitation or inhibition [60], and where several hypotheses have been proposed as a possible mechanism of action [61,62], including the potential role of a local thermal rise [63]. Although the mechanism of action of DBS is not fully understood [61], its efficacy in the treatment of care of ET patients has been demonstrated, whereas the capacity of ultrasound to impact the action tremor in patients, even minimally, remains to be demonstrated.

We present here an exploratory clinical study that evaluates the physiological and clinical effects induced by TUS exposures on the VIM and the DRT on nine (N = 9) essential tremor patients. Different ultrasound stimulation parameters were investigated.

## 2. Methods

### 2.1. Standard protocol approvals, registrations, and patient consents

All patients were enrolled in the ULTRABRAIN Study (clinicaltrial.gov number: NCT04074031 [64]) approved by CPP Ethical Committee (N° IDRCB: 2019-A01791-56). They all gave written informed consent to participate in this study. The patients were scheduled for thalamotomy the same day, immediately after the exploratory neurostimulation study. They were thus prepared for thalamotomy in the neurosurgery department before neurostimulation: they were shaved and equipped with a stereotaxic frame.

### 2.2. Motor evaluations

Tremor was evaluated at baseline using the clinical rating scale for tremor (CRST A-B, range 0–144) developed by Fahn, Tolosa, and Marin [65]. CRST quantifies tremor at rest and upon action of the different body parts, and the kinetic tremor of the upper limbs during writing, drawing, and water pouring.

Tremor severity was evaluated using 3D MR-compatible accelerometers taped on the back of both hands during a standard tremoric posture [66].

Accelerometry data were used to extract the tremor power (in AU) in the 2–20 Hz band [67,68]. More details about the methodology are available in the Supplementary information.

### 2.3. Anatomical targeting

For targeting, anatomical T1-weighted MP2RAGE sequences and diffusion tensor imaging fiber tracking (DTI-FT) were acquired during the inclusion visit on a Siemens Prisma 3 T using a 64-channel head coil for each patient. MP2RAGE imaging parameters were: TE = 2.03 ms, TR = 5000 ms, flip angles = 4°/5°, TIs = 700 ms/2500 ms, slice thickness = 1 mm with an isotropic voxel size. Diffusion imaging parameters were: TE = 89.2 ms, TR = 3230 ms, flip angle = 78°, EPI factor = 128, $b_{max}$ = 3000 s mm$^{-2}$, number of directions = 98, slice thickness of 1.5 mm with an isotropic voxel size.

The location of the VIM target was determined by the neurosurgeon using the Guiot atlas [69], by determining the position of the anterior commissure (AC), posterior commissure (PC) and the midline on the T1-weithted images. The DRT target was determined following the methodology described previously [70]. This target was defined as the barycenter of the DRT in the AC-PC intercommissural plane. The position of the two targets is shown in Fig. 2d.

### 2.4. Neuromodulation protocol

We used the Insightec Exablate Neuro device [72,73] to apply low-power sonication. The system includes a 15 cm radius hemispherical 1024 element array operated at 650 kHz. For the installation of the patient and the positioning of the ultrasonic transducer, we followed the Insightec procedure [74]. Briefly, after the patient was installed on the scanner bed, the transducer was filled with water. First, a T1-weighted anatomical brain image was acquired to locate AC, PC and the midline. Based on the Guiot atlas previously described [69], the VIM position in the AC-PC frame was marked on the Insightec WorkStation (WS) software. The probe was then mechanically positioned so that its geometrical center coincided with the VIM. To correct slight mechanical errors, a few alignment sonications were performed to place the focal spot electronically on the VIM. Two to five alignment sonications were necessary to align the focused beam with the target precisely.

After the alignment procedure, patients received non-thermal, low-power sonications, targeting either the VIM, or the DRT, with four different sonication patterns, and with each pulse lasting less than 30 ms (see Table 1). The dominant hand only was targeted. The pulsing patterns were applied in a blind order for both the patient and the neurologist. All sonications were performed using the Insightec aberration correction for transcranial focusing [75]. The timing of the sonications was recorded using the trigger of the Insightec front-end (FE) unit. The timeline (patient posture and release) was timestamped by the neurologist by pressing a dedicated button inside the MR-room as shown in Fig. 1. After each sonication the neurologist assessed the tremor. In some cases, the effect was weak and inconspicuous, so that the following sonication could be performed rapidly. However, in instances where the tremor significantly decreased, the next sonication was delivered upon the re-occurrence of the tremor. In the case of sustained tremor decrease, the neuromodulation protocol was suspended, and the thermal ablation procedure to treat the ET with high intensity focused ultrasound was performed on the VIM as previously described in the literature [5,73,76–78]. The ablation procedure was performed on all patients, even the ones who did not exhibit a sustained tremor decrease at the end of the neuromodulation session. The overall workflow (low intensity investigational study followed by the CE approved thermal treatment) was carefully explained to the patients. The neurosurgeon systematically warned the neurologist and the patient before switching to the treatment as high power ultrasound were expected to induce transient but uncomfortable side effects (nausea, vertigo, scalp tingling, … [5]).

### 2.5. TUS parameters

All stimulation patterns lasted 35s and were composed of three 5s bursts followed by a 10s off period, except for Mode 4 which consisted of a series of 9 spots distributed on a 0.75 mm × 0.75 mm grid around the initial target, in the transverse plane with a total duration of 54s. Only the duration and the pulse repetition frequency (PRF) of the bursts varied between the different patterns. The sonication patterns were derived from published works [38,79] and are summarized in Table 1. Mode 1 and 2 correspond to two different ways to achieve a high duty cycle (one-third of the time) with either a long duration and a low pulse repetition frequency (mode 1) or a short duration and a high pulse repetition frequency (mode 2). Mode 3 and 4 correspond to a low duty cycle (5 %), either on one target point only or on a grid of 9 points including the central target and 8 neighbors within a 1.5 mm square. The exact order of the successive stimulations was not imposed in our exploratory protocol. Our goal was to investigate whether TUS could decrease the tremor in a DBS-like manner. As the gold standard in ET is VIM DBS, it was decided to use preferentially the following order: 1) stimulate the VIM with the first three sonication modes, starting with the high duty cycle modes 2) move to the DRT and test the last sonication used in the VIM to change one parameter only (the target) 3) use the multi-targeted mode 4 to cover a larger stimulation zone.

The Exablate Neuro device used here included dedicated pulse sequences implemented specifically for this study. Such sequences are currently not available in the CE-approved Exablate Neuro system.

The electrical power applied to the ultrasonic transducer was

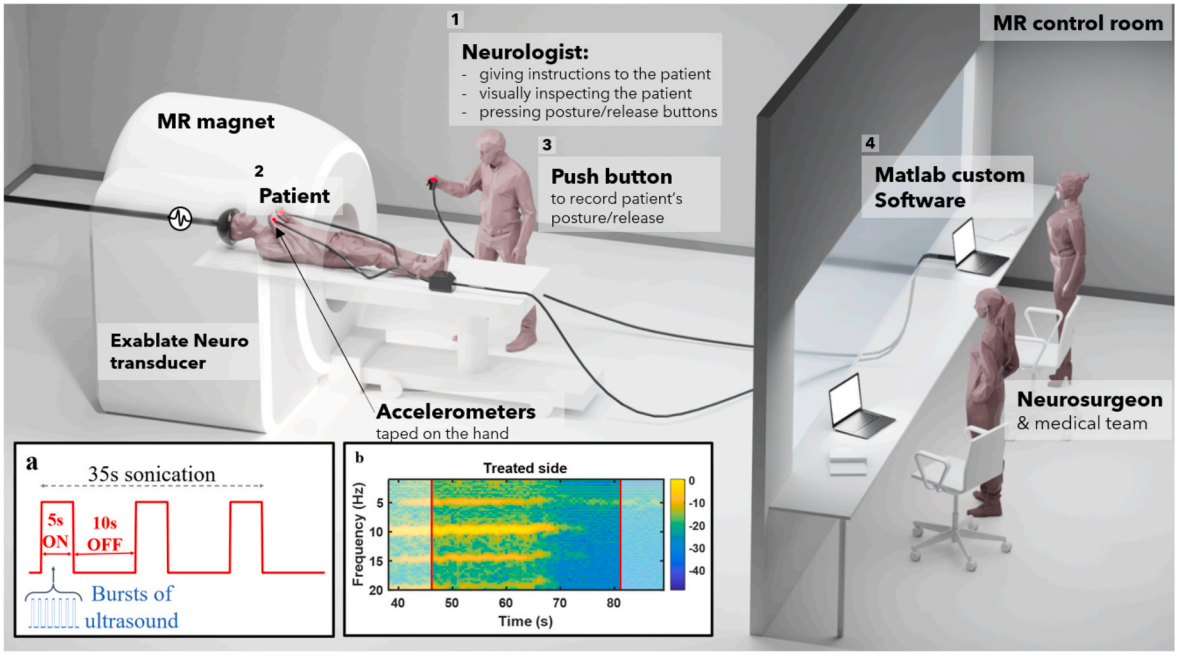


**Fig. 1.** Diagram of the neuromodulation apparatus during the procedure. **1.** The neurologist asks the patient to hold a posture before the sonication starts. **2.** The patient inside the MR tunnel follows the neurologist's instructions. **3.** When the posture is held, the neurologist presses a push button to record when the patient has started to hold it. **4.** Accelerometers' data, timestamps from the posture/release tasks and Insightec's triggers are recorded using customized Matlab software inside the MR control room. **(a)** Neuromodulation pattern. All neuromodulation sonications consisted of three 5s bursts followed by a 10s period OFF. The burst characteristics changed depending on the neuromodulation sequences. **(b)** Spectrogram during TUS. The red vertical bars highlight the beginning and the end of the sonication. (For interpretation of the references to color in this figure legend, the reader is referred to the Web version of this article.)

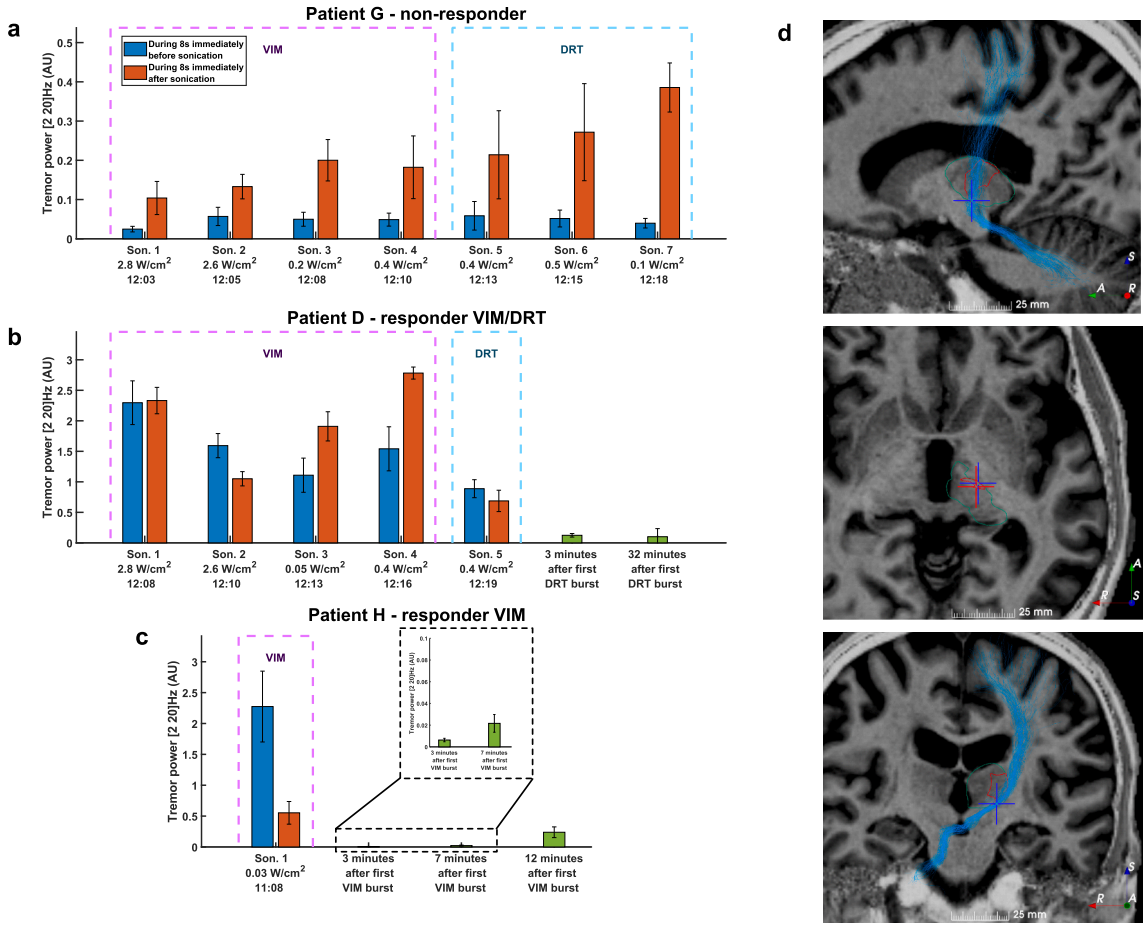


**Fig. 2.** ***(a-c)*** *Tremor power immediately before and after each TUS for patients G, D and H respectively. Blue bars correspond to the average of the tremor power during the 8s preceeding the stimulation and orange bars to the average of the tremor power during the 8s following the stimulation. Green bars correspond to post-neuromodulation measurements. The error bars correspond to the standard deviation during the measurement time interval.* ***(d)*** *Position of the VIM (red cross) and DRT (blue cross) targets. The DRT target corresponded to the barycenter of the fibers (in light blue) going from the dental superior nucleus to the primary motor cortex. The green and red overlay delineate the thalamus and the VIM respectively using the volBrain open-source software* [71]. (For interpretation of the references to color in this figure legend, the reader is referred to the Web version of this article.)

adjusted to produce an acoustic pressure of ~0.8 MPa at the target inside the brain, corresponding to a spatial-peak pulse average intensity ($I_{sppa}$) of 19.8 W/cm$^2$. More information about the methodology for determining the power adjustment is provided in the Supplementary information. For patients A to E and patient G, the first four sonications targeted the VIM, and the last sonication targeted the DRT. For each patient, a lower power sonication was introduced within the neuromodulation sequences, except for patient C (due to technical reasons). For patient F, the same procedure was applied except that the third sonication, which was the lower power one, was repeated twice due to a technical error preventing tremor recording during the first occurrence. For patient H, the VIM was targeted with a unique low power sonication and a low duty cycle mode which caused an important decrease of the tremor. For patient I, only the DRT was sonicated twice using a low duty cycle mode. The sonications performed for each patient are detailed on Table 3.

### 2.6. Tremor acquisition and analysis

Before sonications, once patients were installed on the scanner bed with the stereotactic frame attached to the bed but before entering the MR tunnel, the baseline tremor was recorded. Patients were asked by the neurologist to hold a postural tremor for approximately 30s.

During each neuromodulation sequence, the tremor was also recorded as the patient held and released a batwing tremoric posture [66] as instructed by the neurologist (Fig. 1). To evaluate the tremor change during each sonication, the average tremor power was computed over the 8s before the beginning of each sonication (see supplementary materials for details), and the 8s after the end of each sonication. Post-neuromodulation effects were measured in the 7- to 33-min period following the end of the relevant sequence for the short-lived, and extended-duration respectively. The fundamental tremor frequency immediately before and after each sonication was also measured.

### 2.7. Temperature monitoring during stimulation

The temperature was monitored inside the patient's brain with the manufacturer's MR thermometry sequences during the sonications [80].

### 2.8. Statistical analysis

A statistical analysis was performed to assess the immediate effect of the sonications on the tremor power of patients A to G. Mean tremor power values immediately before and after the sonication were log-

**Table 1**
Sonication patterns tested.

| Sonication mode 1 | | | | | | |
|---|---|---|---|---|---|---|
| | Duration | Ramp duration | Ramp shape | Repetition interval/ frequency | Duty cycle | Notes |
| Pulse | 30 ms | 0s | rectangular | 100 ms/10 Hz | 30 % | |
| Pulse train | 5s | 0s | rectangular | 15s/0.0667 Hz | | |
| Pulse train repeat | 35s | 0s | rectangular | N/A | | |
| **Sonication mode 2** | | | | | | |
| | Duration | Ramp duration | Ramp shape | Repetition interval/ frequency | Duty cycle | Notes |
| Pulse | 2 ms | 0s | rectangular | 5.98 ms/167 Hz | 33.4 % | |
| Pulse train | 5s | 0s | rectangular | 15s/0.0667 Hz | | |
| Pulse train repeat | 35s | 0s | rectangular | N/A | | |
| **Sonication mode 3** | | | | | | |
| | Duration | Ramp duration | Ramp shape | Repetition interval/ frequency | Duty cycle | Notes |
| Pulse | 2 ms | 0s | rectangular | 40 ms/25 Hz | 5 % | |
| Pulse train | 5s | 0s | rectangular | 15s/0.0667 Hz | | |
| Pulse train repeat | 35s | 0s | rectangular | N/A | | |
| **Sonication mode 4** | | | | | | |
| | Duration | Ramp duration | Ramp shape | Repetition interval/ frequency | Duty cycle | Notes |
| Pulse | 2 ms | 0s | rectangular | 40 ms/25 Hz | 5 % | This sequence is applied for 1s successively on 9 points forming a 1.5 × 1.5 mm grid |
| Pulse train | 1s | 0s | rectangular | 9s/0.111 Hz | | |
| Pulse train repeat | 54s | 0s | rectangular | N/A | | |

transformed beforehand, and two-tailed paired sample Student's t-tests were conducted (n = 7 for each sonication except for mode 2 sonication of the VIM for which n = 6 due to a technical issue for patient E). To assess the impact of each sonication mode, mean tremor powers displayed in Fig. 2a–c and Fig. S2 for patients A to G were pooled with matched respective power, sonication mode and target (Table 3), e.g. all sonications targeting the VIM with a power of 2.6 W/cm$^2$ and sonication mode n°1 were pooled together. In Table 3, grouped sonications are indicated with cells having the same background color (except for cells with a red background, which indicates that an error occurred during the sonication, and therefore that the sonication was not considered in the statistical analysis). Since only a restricted set of patients underwent more than five recorded sonications, the statistical analysis was not performed on sonication 6, 7 and 8 (except for patient F whose sixth sonication was considered because a technical issue induced a shift in the ordering of the sonications). The significance level was initially chosen as $\alpha = 0.05$ and since four tests were done, a Bonferroni correction was applied, decreasing the significance level to an effective level $\alpha_{\text{Bonferroni}} = 0.0125$. For each such statistical test, we also performed a Wilcoxon signed-rank test to assess the robustness of the finding. Results of non-parametric tests are reported only if they do not align with t-tests (i.e one test is significant while the other is not). Cohen's *d* values are reported to assess the effect size. Patients A, B and D who are three responders which underwent similar sonication patterns and for which post-neuromodulation measurements were performed at two different times were grouped together and the data shown in Fig. 3b were log-transformed. Such data were then used in a repeated measures ANOVA, followed by Tukey's HSD post-hoc tests to assess if significant differences could be found between the tremor power at different times. In this case, $\alpha = 0.05$.

## 3. Results

### 3.1. Participants

Nine patients with ET, refractory to medical treatments and eligible for TUS thalamotomy were included in this study and accepted for treatment with the Insightec's Exablate Neuro Magnetic Resonance-guided Focused Ultrasound (MRgFUS) device [72,73] at the Paris Brain Institute (ICM, Paris, France). Demographical, clinical, and radiological data are summarized in Table 2.

### 3.2. Tremor power before, during and after TUS

The sonication details together with the corresponding estimates of pressures and intensities applied to each patient are summarized in Table 3.

The spectrogram in Fig. 1b highlights the impact of the stimulation on the frequency components of the tremor. It was acquired on Patient C. The decrease in tremor did not start at the beginning of the stimulation (red vertical bar) but took 25s to start.

For each patient, and for each stimulation, the average tremor powers were computed over the 8s before the beginning of each sonication and 8s after the end of each sonication (transparent windows on each side of Fig. 1b). The tremor power was modulated differently depending on the TUS mode. The results of the statistical analysis of the mean tremor power immediately after stimulation are: for mode 2 VIM sonication t (n = 5) = −0.81, p = 0.46, $d = -0.20$; for mode 1 VIM sonication: t (n = 6) = −0.46, p = 0.66, $d = -0.13$; for mode 3 VIM sonication: t (n = 6) = −2.47, $p_{\text{t-test}} = 0.049 > \alpha_{\text{Bonferroni}}$ and $p_{\text{Wilcoxon}} = 0.078 > \alpha_{\text{Bonferroni}}$, $d = -0.33$; for mode 3 first DRT sonication: t (n = 6) = 0.37, p = 0.72, $d = 0.18$. Of note, negative values of *d* reflect an

**Table 2**
Characteristics of the nine patients.

| | Patient A | Patient B | Patient C | Patient D | Patient E | Patient F | Patient G | Patient H | Patient I |
|---|---|---|---|---|---|---|---|---|---|
| Age (years) | 59 | 46 | 79 | 65 | 69 | 57 | 75 | 69 | 72 |
| Gender | Male | Male | Male | Female | Female | Male | Male | Male | Male |
| Treated hand | right | left | right | right | right | right | right | left | right |
| *CRST A-B at inclusion* | 26 | 33 | 32 | 37 | 52 | 23 | 31 | 25 | 41 |
| *CRST A-B* 1 month *after the ablative treatment* | 13 | 16 | 19 | 18 | 22 | 15 | 20 | 11 | 26 |
| *Change in CRST A-B between inclusion and* 1 month *after the ablative treatment (%)* | 50.0 % | 51.5 % | 40.6 % | 51.4 % | 57.7 % | 34.8 % | 35.5 % | 56.0 % | 36.6 % |
| AC-PC VIM location (Guiot Atlas) (mm) | [14,0; 7,0; 0,0] | [-14,2; 6,0; 0,5] | [14; 6,5; 0,0] | [15,0; 6,5; 0,0] | [14,0; 6,0; 0,0] | [14,0; 6,5; 0,0] | [14,0; 7,0; 0,0] | [-15,0; 6,5; 0,0] | [14,5; 7,5; 0,5] |
| AC-PC DRT location (mm) | [15,0; 5,0; 0,0] | [-12,5; 5,0; 0,5] | [12,0; 6,0; 0,0] | [15,5; 8,0; 0,0] | [14,0; 3,5; 0,0] | [15,0; 6,0; 0,0] | [12,5; 6,0; 0,0] | [-14,5; 5,5; −1,0] | [15,5; 6,0; 0,5] |

increase of tremor power. None of the sonication modes had a statistically significant effect on the tremor power immediately after the end of the sonication once Bonferroni correction was applied.

Nevertheless, noticeable decreases or increases of the tremor power could be observed after certain sonications at the individual scale. The overall response differed from patient to patient. 55 % were responders (patients A, B, C, D and H), and 45 % were non-responders (patients E, F, G and I) patients. The main results are displayed (Fig. 2a-c) and described for all patients in the supplementary materials (Fig. S2). Typically, non-responders (Fig. 2a) exhibited an increase of tremor power at the end of the stimulation compared to the beginning of the stimulation: this was the case for all sonications for patients E, F and G. Responders typically showed a large and sustained decrease in tremor, which prevented further sonications either after sonication in the VIM only (patient H in Fig. 2c) or after switching from VIM stimulation to DRT stimulation (patients A, B, C, D). Patient D is displayed in Fig. 2b.

The fundamental tremor frequency immediately before and after each sonication was 5.17 ± 0.62 Hz and 5.01 ± 0.66 Hz corresponding to a relative fundamental frequency change of −0.16 ± 0.41 Hz. It is to be noted that the spectrogram frequency resolution was 0.167 Hz. The details for each sonication is available in Table S2.

### 3.3. Post-neuromodulation effects

Post-neuromodulation measurements occurred in patients A to D and H only due to time constraints with the clinical workflow of the ultrasound thalamotomy that was planned with the Exablate Neuro immediately after the ultrasound neurostimulation. Sustained effects prevented from continuing the scheduled stimulations in patients B, C and D after a combination of 4–5 stimulations in the VIM followed by a stimulation in the DRT with a low duty cycle (5 %). Patient H exhibited a 93.4 % decrease from baseline tremor 3 min after the first VIM stimulation with a low duty cycle (5 %), and a 77.2 % decrease after 7 min. Short-lived post-neuromodulation effects were observed after DRT neuromodulation for all the patients whose tremor was measured in this 3–7 min timeframe after stimulation: the reduction in tremor power was higher than 90 % (Fig. 3b). For patients C and D, the tremor power remained lower than 5 % of the baseline, up to 26 min and 33 min respectively (Table 3). Patients C and D both self-reported that the tremor was gone and thought that the ablative clinical treatment had been performed. The repeated measures ANOVA performed on baseline and post-neuromodulation measurements for patients A, B and D reported in Fig. 3b indicate a statistically significant effect of time on tremor power: $F(2,4) = 7.51$, $p = 0.044$, $\eta^2 = 0.79$. Tukey's HSD test comparing baseline with short-lived post-neuromodulation measurements was also significant: $p = 0.048$, $d = 2.70$, but not baseline compared with extended-duration post-neuromodulation measurements: $p = 0.40$, $d = 1.33$, nor short-lived measurements compared with extended-duration measurements: $p = 0.37$, $d = -1.63$.

For patient D, we continued to record baseline tremors every 5 min (Fig. 3a).

### 3.4. Thermal rise during TUS

No heating was seen on the MR thermometry images for any of the neuromodulation sonications. Overall, the temperature at target during sonication was 37.2 ± 1.4 °C compared to 36.8 ± 1.4 °C for a control voxel located 3 cm away from the target. The temperature for each patient is provided in Table 4.

## 4. Discussion

### 4.1. Target engagement by neuromodulation

This study demonstrates the possibility for MR-guided low-intensity focused ultrasound waves to elicit a large motor response (more than 98

**Table 3**
Sonication details for each patient. For patients B, C, D and H, the sustained decrease of the tremor was too strong to allow ultrasound neurostimulation to continue. Red cells correspond to sonication interrupted due to MR noise (patient C and E) or a technical issue which prevented tremor recording during that sonication (patient F). Other background colors correspond each to the pooling which is considered for the statistical analysis described in the methods section.

| | Sonication 1 | Sonication 2 | Sonication 3 | Sonication 4 | Sonication 5 | Sonication 6 | Sonication 7 | Sonication 8 |
|---|---|---|---|---|---|---|---|---|
| **Patient A** | | | | | | | | |
| ISPTA (W/cm²) | 2.8 | 2.6 | 0.0 | 0.4 | 0.4 | 0.1 | 0.6 | N/A |
| Pressure (MPa) | 0.80 | 0.80 | 0.00 | 0.80 | 0.79 | 0.81 | 0.94 | N/A |
| Location | VIM | VIM | VIM | VIM | DRT | DRT | DRT | N/A |
| Sonication mode | 2 | 1 | 3 | 3 | 3 | 4 | 3 | N/A |
| **Patient B** | | | | | | | | |
| ISPTA (W/cm²) | 2.8 | 2.6 | 0.0 | 0.4 | 0.4 | 0.1 | sustained effect | sustained effect |
| Pressure (MPa) | 0.80 | 0.80 | 0.00 | 0.80 | 0.80 | 0.80 | sustained effect | sustained effect |
| Location | VIM | VIM | VIM | VIM | DRT | DRT | sustained effect | sustained effect |
| Sonication mode | 2 | 1 | 1 | 3 | 3 | 4 | sustained effect | sustained effect |
| **Patient C** | | | | | | | | |
| ISPTA (W/cm²) | 2.8 | 0.8 | 2.6 | 0.4 | 0.4 | sustained effect | sustained effect | sustained effect |
| Pressure (MPa) | 0.80 | 0.80 | 0.80 | 0.80 | 0.80 | sustained effect | sustained effect | sustained effect |
| Location | VIM | VIM | VIM | VIM | DRT | sustained effect | sustained effect | sustained effect |
| Sonication mode | 2 | 1 | 1 | 3 | 3 | sustained effect | sustained effect | sustained effect |
| **Patient D** | | | | | | | | |
| ISPTA (W/cm²) | 2.8 | 2.6 | 0.05 | 0.4 | 0.4 | sustained effect | sustained effect | sustained effect |
| Pressure (MPa) | 0.80 | 0.80 | 0.28 | 0.80 | 0.79 | sustained effect | sustained effect | sustained effect |
| Location | VIM | VIM | VIM | VIM | DRT | sustained effect | sustained effect | sustained effect |
| Sonication mode | 2 | 1 | 3 | 3 | 3 | sustained effect | sustained effect | sustained effect |
| **Patient E** | | | | | | | | |
| ISPTA (W/cm²) | 1.9 | 2.6 | 0.1 | 0.4 | 0.4 | 0.7 | N/A | N/A |
| Pressure (MPa) | 0.80 | 0.80 | 0.17 | 0.80 | 0.80 | 0.99 | N/A | N/A |
| Location | VIM | VIM | VIM | VIM | DRT | DRT | N/A | N/A |
| Sonication mode | 2 | 1 | 1 | 3 | 3 | 3 | N/A | N/A |
| **Patient F** | | | | | | | | |
| ISPTA (W/cm²) | 2.8 | 2.6 | 0.02 | 0.02 | 0.4 | 0.4 | 0.4 | 0.1 |
| Pressure (MPa) | 0.80 | 0.80 | 0.18 | 0.18 | 0.80 | 0.81 | 0.81 | 0.81 |
| Location | VIM | VIM | VIM | VIM | VIM | DRT | DRT | DRT |
| Sonication mode | 2 | 1 | 3 | 3 | 3 | 3 | 3 | 4 |
| **Patient G** | | | | | | | | |
| ISPTA (W/cm²) | 2.8 | 2.6 | 0.2 | 0.4 | 0.4 | 0.5 | 0.1 | N/A |
| Pressure (MPa) | 0.80 | 0.81 | 0.22 | 0.81 | 0.81 | 0.91 | 0.91 | N/A |
| Location | VIM | VIM | VIM | VIM | DRT | DRT | DRT | N/A |
| Sonication mode | 2 | 1 | 1 | 3 | 3 | 3 | 4 | N/A |
| **Below this line, low duty cycle only** | | | | | | | | |
| **Patient H** | | | | | | | | |
| ISPTA (W/cm²) | 0.03 | sustained effect | | | | | | |
| Pressure (MPa) | 0.19 | sustained effect | | | | | | |
| Location | VIM | sustained effect | | | | | | |
| Sonication mode | 3 | sustained effect | | | | | | |
| **Patient I** | | | | | | | | |
| ISPTA (W/cm²) | 0.4 | 0.6 | | | | | | |
| Pressure (MPa) | 0.80 | 0.93 | | | | | | |
| Location | DRT | DRT | | | | | | |
| Sonication mode | 3 | 3 | | | | | | |

% in one patient) sustained for several minutes (up to 30 min in one patient). Although the response varied from patient to patient, the effect of ultrasound neurostimulation was more pronounced than anything previously reported in humans.

Pre-clinical studies in rodents have demonstrated motor responses to TUS via EMG recordings. Tufail et al. [29] demonstrated EMG spikes after TUS in the motor cortex with a 92 % success rate, as well as an increased multi-unit activity. King et al. [28,54] confirmed these findings and explored a wide range of frequencies (250 kHz–600kHz) and acoustic intensities (0.1–16.8 W/cm$^2$). The closest set of parameters to the ones used in our study (0.3 W/cm$^2$ at 600 kHz) yielded to 20 % response rate. We report here 55 % of responders, with an average number of 5.2 neuromodulations per patient. More recently, Sharabi et al. [35] tested the impact of stimulating the inferior olivary nucleus in a rat model of essential tremor. The authors exhibited a reduction of EMG spikes over approximately 70s with TUS parameters of DC = 3.3 %, PRF = 0.3 Hz, Isppa = 27.2 W.cm$^{-2}$ and f = 320 kHz. Our study echoes these findings and provides the first evidence of motor response after TUS in patients suffering from Essential Tremor.

Recent studies investigated motor response in healthy volunteer when targeting the motor cortex (M1) [81–89]. Each study exhibited a change in the motor evoked potentials (MEP) amplitudes following a stimulation of the motor cortex, and one study highlighted an influence of duty cycle on inducing an inhibitory or excitatory effect on M1 [88].

a

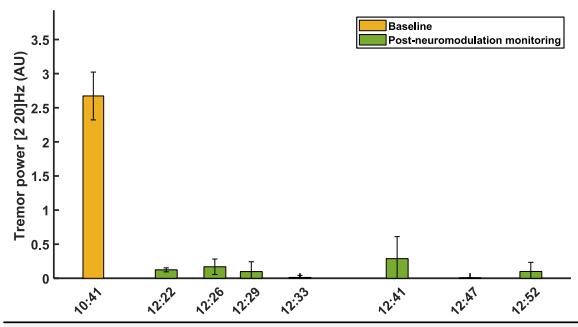


b

| | | Patient A | Patient B | Patient C | Patient D |
|---|---|---|---|---|---|
| Baseline Tremor power (AU) | | 0.36 ± 0.26 | 2.28 ± 0.21 | 0.53 ± 0.27 | 2.67 ± 0.35 |
| Short-lived post-neuromodulation effects | Tremor power (AU) | 0.03 ± 0.02 (T = 3 min) | 0.03 ± 0.01 (T = 7 min) | Not measured | 0.12 ± 0.03 (T = 3 min) |
| | Tremor power reduction from baseline | 90.7% | 98.5% | --- | 95.4% |
| Extended duration post-neuromodulation effects | Tremor power (AU) | 0.41 ± 0.29 (T = 13 min) | 0.40 ± 0.12 (T = 23 min) | 0.009 ± 0.008 (T = 26 min) | 0.10 ± 0.13 (T = 33 min) |
| | Tremor power reduction from baseline | -14.6% | 82.3% | 98.4% | 96.2% |

**Fig. 3. (a)** Baseline tremor power for patient D 3 min after the 5th stimulation that occurred at 12:19, and approximately every 5 min over 30 min, compared to the baseline. The error bars correspond to the standard deviation during the measurement time interval **(b)** Tremor power reduction for patient A to D shortly after stimulation and sustained post-neuromodulation effects more than 13 min after stimulation.

Shamli Oghli et al. [86] hypothetized that theta-burst TUS in M1 may induce synaptic plasticity via NMDA receptors and reported a reduction of the ultrasound-induced change in MEP after the administration of brain active drugs ($Ca^{2+}$ and $Na^{+}$ channels blockers). Bilateral ultrasonic neurostimulation of M1 in the context of Parkinson disease patients induced an increase of MEP amplitudes, but no change in the MDS-UPDRS clinical scale was associated with it [90]. Nakajima et al. [89] reported the reaction time to withhold a voluntary hand movement was increased after ultrasound stimulation of the anterior inferior frontal cortex. Our study further investigates the impact of ultrasound stimulation on movement control but targeted deeper brain structures. We report here that only 5 out of 9 patients responded to the ultrasound stimulation despite the use of state-of-the-art targeting combining stereotaxic positioning and medical grade skull aberration correction. Our preliminary results do not demonstrate a correlation of the success of the stimulation with a specific set of acoustic parameters for the stimulation, nor with a specific target. Nevertheless, it is noticeable that all the ET patients who responded best to the thermal ablation (more than 40 % reduction of the CRST score one month after the treatment (Table 2) match with the ultrasound-stimulation responder patients, except for patient E. Of note, patient E happens to be the patient with the most severe tremor score (CRST = 52 before treatment).

### 4.2. Non-thermal mechanism

Transient effects of focused ultrasound on tremor have been reported previously by Elias et al. [73] during MRgFUS treatment of patients suffering from ET. However, such effects were observed when gradually increasing the energy at the target before permanently ablating the target with peak temperatures around 50 °C. Sensory symptoms were also reported for temperatures in the 45°C–50 °C range, at applied powers of 550 W [73]. At such powers, the estimated pulse average intensities at target are of the order of 1500 W $cm^{-2}$ (assuming 5 % energy transmission [91] through the skull). Usually, powers applied for thermal ablation range from 300 to 1000 W [72] ($I_{sppa}$ values ranging between ~1500 and 5500 W $cm^{-2}$).

In contrast, our study was achieved with the same focused ultrasound device as Elias et al. [73] (ExablateNeuro) but operated at its lower power bound. We can reasonably assume that a non-thermal mechanism of action drives the effect of ultrasound on brain activity in our study, leading to reversible tremor changes. This is supported by the lack of significant measured thermal rise during ultrasound stimulation. This was not higher than the noise level of the MR temperature monitoring sequence. This is in line with Constans et al.'s [92] thermoacoustic simulation of four published pre-clinical TUS experiments [22,29,91,92] where the temperature elevation was estimated to be less than 1 °C for acoustic parameters similar to those used in our study. The peak negative pressure at the focus was estimated to be 0.8 Mpa in our study, corresponding to spatial peak pulse average intensities as low as 20 W $cm^{-2}$. This value is close to the recommendation of the FDA for diagnostic ultrasound ($I_{sppa} < 19$ W $cm^{-2}$) [93].

### 4.3. Spatial specificity of the stimulation: DRT and VIM stimulation

VIM neuromodulation produced a large reduction of the tremor for one patient (patient H); DRT stimulation following VIM stimulation produced a large reduction of the tremor for four patients (A to D). In the latter case, a cumulative effect of ultrasound neuromodulation cannot be excluded [49], making it difficult to separate the influence of prior VIM stimulation. This should be considered in the design of future studies. The results of our exploratory study suggest that there should be at least 30-min wait before testing a different set of stimulation parameters used here.

It is also worth noting that the VIM and the DRT differ anatomically: a nucleus with large, heterogeneous and clumped cells for the VIM [94] versus a white matter fiber bundle formed by efferent fibers from the dentate nucleus projecting toward the red nucleus and innervating the ventral lateral nucleus of the thalamus for the DRT. It could explain the different neurophysiological response to ultrasound stimulation. Similar effects on tremor have been reported after DRT or VIM DBS [95,96]. Dembeck et al. showed that VIM-DBS efficiency was dependent on the target distance from the DRT [97], with better results for a DBS location closer to the DRT. We believe that the precision of the targeting enabled by the Insightec's large aperture multi-element transducer was appropriate for investigating VIM vs DRT neuromodulation. At 650 kHz, with a hemispherical array using a CT-based correction for patient skull aberration [21,75,98], the estimated focal spot size inside the brain is 1.5 mm wide and 3.0 mm long [74,75], providing more precise targeting than previous studies of TUS on humans [48–50,99,100]. In our patients, the distance between the VIM and the DRT was 1.8 ± 0.4 mm, which was slightly larger than the lateral resolution of the focal spot (1.5 mm). This suggests that the ultrasonic accuracy was sufficient to specifically target either the DRT or the VIM.

Previous pre-clinical studies in non-human primates reported the spatial specificity of TUS. Deffieux et al. [42] reported significant

**Table 4**
Average thermal rise for each patient.

| | Patient A | Patient B | Patient C | Patient D | Patient E | Patient F | Patient G | Patient H | Patient I |
|---|---|---|---|---|---|---|---|---|---|
| Temperature at target (°C) during sonication | 37.2 ± 0.4 | 37.1 ± 0.5 | 37.4 ± 2.2 | 36.8 ± 0.4 | 36.6 ± 3.1 | 37.7 ± 1.2 | 37.2 ± 0.7 | 37.7 ± 0.7 | 37.0 ± 0.2 |
| Temperature at a control voxel 3 cm away from the target (°C) during sonication | 37.1 ± 0.4 | 36.9 ± 0.9 | 36.2 ± 1.9 | 37.2 ± 0.4 | 36.0 ± 3.1 | 36.8 ± 0.7 | 37.4 ± 0.9 | 36.9 ± 0.5 | 37.0 ± 0.1 |

anti-saccade latency change in the case of frontal eye field stimulation and no significant change for premotor cortex stimulation in non-human primates. Folloni et al. [44] investigated the effect of TUS on the coupling of amygdala activity with activity in other brain areas. They reported that the coupling of amygdala activity was significantly changed after amygdala ultrasound stimulation but not after anterior cingulate cortex (ACC) ultrasound stimulation, except that ACC stimulation led to an alteration in amygdala coupling with ACC. Finally, Verhagen et al. [43] stimulated different cortical areas and reported changes in functional connectivity in the targeted regions only.

### 4.4. Sustained post-neuromodulation effect

A sustained effect was observed in five patients (A, B, C, D and H) and maintained for up to 30 min for one patient (patient D).

Sustained post-neuromodulation effects have been reported in animal models. Verhagen et al. [43] stimulated the supplementary motor area and the fronto-polar-cortex over 45s, with an imposed pressure at the target of 0.88 MPa, 30 ms pulse duration and 10 Hz PRF (leading to a 30 % DC). They showed sustained reversible changes in the connectivity of the stimulated regions compared to the resting-state fMRI for more than 2 h. With the same parameters, but with a total sonication time reduced from 45s to 20s, Pouget et al. [79] demonstrated a 30min post-neuromodulation effect on saccade/anti-saccade latencies when stimulating the frontal eye field. In this study, the choice of the ultrasound stimulation parameters for mode 1 and 2 was based on previous work on sustained functional changes after TUS in primates [43] whereas the choice of the ultrasound stimulation parameters for mode 3 was based on the results obtained by the group of Seung-Schik Yoo to suppress SEP in rabbits [38] for 7 min, and to decrease seizure bursts in mice [36].

Due to the time constraints associated with performing ultrasonic thalamotomy to permanently suppress tremor, the effect of post-neuromodulation could not be monitored over time for patients who witnessed a remarkable decrease of their tremor (patients A to D and H). We could not wait until the tremor returned to its pre-therapeutic severity, but only until tremor reappeared, and was severe enough to be assessed, and the patient could provide feedback on his tremor during the dose escalation leading to thermal ablation of the target. Further experiments outside the workflow of an actual treatment have to be performed to better quantify post-neuromodulation effects and placebo-control should be added to rule out possible placebo effect.

Further experimental work is needed to test other sonication patterns with different duty cycles, pulse duration, stimulation time, and pressures at the target to improve understanding of TUS parameters. The Exablate Neuro device could be used to test different types of stimulations in healthy volunteers, provided that a frameless head holder is developed. Alternatively, neuronavigated transducers could be used to perform such experiments. To achieve the same precision in terms of focal spot dimensions, either multi-element arrays [101] or acoustic lenses [19] are good candidates. Increasing the frequency could lead to higher precision targeting [102,103] if precise aberration corrections are applied.

Overall, this study reports on the feasibility of inducing a substantial reduction of the tremor power with MR-guided low-energy focused ultrasound stimulation in ET patients, with up to 98 % tremor reduction 3 min after sonication that lasted up to 33 min. No significant thermal rise occurred at the target, supporting a non-thermal mechanism. However, even though the precision of targeting was optimized with a state-of-the-art setup (head shaving, stereotactic frame, clinically validated aberration correction), response variability was observed and remains to be explained.

## Funding

This work was achieved in collaboration and with the financial support of Insightec ltd. This work was supported by the Bettencourt Schueller Foundation and the "Agence Nationale de la Recherche" under the program ‘‘Future Investments’’ with the reference ANR-10-EQPX-15. The work was performed with the support of the ART (Technological Research Accelerator) biomedical ultrasound program of INSERM and the Focused Ultrasound Foundation Center of Excellence program (Physics for Medicine Paris).

## Data availability

Anonymized participant data can be made available upon requests directed to the corresponding author. Proposals will be reviewed on the basis of scientific merit, ethical review, available resources and regulatory requirements. After approval of a proposal, anonymized data will be made available for reuse. A steering committee will have the right to review and comment on any draft papers based on these data before publication.

## CRediT authorship contribution statement

**Thomas Bancel:** Writing – review & editing, Writing – original draft, Software, Methodology, Investigation, Formal analysis, Conceptualization. **Benoît Béranger:** Writing – review & editing, Software, Data curation, Conceptualization. **Maxime Daniel:** Writing – review & editing, Visualization, Software, Formal analysis. **Mélanie Didier:** Writing – review & editing, Software, Methodology, Formal analysis. **Mathieu Santin:** Writing – review & editing, Methodology, Investigation. **Itay Rachmilevitch:** Writing – review & editing, Software. **Yeruham Shapira:** Writing – review & editing, Project administration, Funding acquisition. **Mickael Tanter:** Writing – review & editing, Funding acquisition, Conceptualization. **Eric Bardinet:** Writing – review & editing, Project administration, Methodology. **Sara Fernandez Vidal:** Writing – review & editing, Software, Methodology, Formal analysis. **David Attali:** Writing – review & editing, Validation, Methodology, Conceptualization. **Cécile Galléa:** Writing – review & editing, Methodology, Investigation. **Alexandre Dizeux:** Writing – review & editing, Visualization. **Marie Vidailhet:** Writing – review & editing, Validation, Methodology, Conceptualization. **Stéphane Lehéricy:** Writing – review & editing, Project administration, Methodology, Funding acquisition, Conceptualization. **David Grabli:** Writing – review & editing, Investigation, Conceptualization. **Nadya Pyatigorskaya:** Writing – review & editing, Supervision, Methodology, Investigation, Conceptualization. **Carine Karachi:** Writing – review & editing, Investigation, Conceptualization. **Elodie Hainque:** Writing – original draft, Methodology, Investigation, Conceptualization. **Jean-François Aubry:** Writing – review & editing, Validation, Project administration, Methodology, Investigation, Funding acquisition, Conceptualization.

## Declaration of competing interest

The authors declare the following financial interests/personal relationships which may be considered as potential competing interests:

IR and YS are employees of Insightec. JFA received a research grant from Insightec for preclinical work on transcranial ultrasound.

## Acknowledgments

This work was achieved in collaboration and with the financial support of Insightec ltd, to which we are grateful. This work was supported by the Bettencourt Schueller Foundation and the "Agence Nationale de la Recherche" under the program ‘‘Future Investments’’

with the reference ANR-10-EQPX-15. The work was performed with the support of the ART (Technological Research Accelerator) biomedical ultrasound program of INSERM and the Focused Ultrasound Foundation Center of Excellence program (Physics for Medicine Paris). The authors thank Anais Hervé, Clémentine Trosch, and Vincent Degos for patient care.

## Appendix A. Supplementary data

Supplementary data to this article can be found online at https://doi.org/10.1016/j.brs.2024.05.003.

## References

[1] E. D. Louis, M. McCreary, How common is essential tremor? Update on the worldwide prevalence of essential tremor. Tremor Hyperkinetic Mov. 11, 28.
[2] Haubenberger D, Hallett M. Essential tremor. N Engl J Med 2018;378:1802–10.
[3] Louis ED. Essential tremor. Lancet Neurol 2005;4:100–10.
[4] Lozano AM, Lipsman N, Bergman H, Brown P, Chabardes S, Chang JW, Matthews K, McIntyre CC, Schlaepfer TE, Schulder M, Temel Y, Volkmann J, Krauss JK. Deep brain stimulation: current challenges and future directions. Nat Rev Neurol 2019;15:148–60.
[5] Elias WJ, Lipsman N, Ondo WG, Ghanouni P, Kim YG, Lee W, Schwartz M, Hynynen K, Lozano AM, Shah BB, Huss D, Dallapiazza RF, Gwinn R, Witt J, Ro S, Eisenberg HM, Fishman PS, Gandhi D, Halpern CH, Chuang R, Butts Pauly K, Tierney TS, Hayes MT, Cosgrove GR, Yamaguchi T, Abe K, Taira T, Chang JW. A randomized trial of focused ultrasound thalamotomy for essential tremor. N Engl J Med 2016;375:730–9.
[6] Bronstein JM, Tagliati M, Alterman RL, Lozano AM, Volkmann J, Stefani A, Horak FB, Okun MS, Foote KD, Krack P, Pahwa R, Henderson JM, Hariz MI, Bakay RA, Rezai A, Marks WJ, Moro E, Vitek JL, Weaver FM, Gross RE, DeLong MR. Deep brain stimulation for Parkinson disease: an expert consensus and review of key issues. Arch Neurol 2011;68. https://doi.org/10.1001/archneurol.2010.260.
[7] Flora ED, Perera CL, Cameron AL, Maddern GJ. Deep brain stimulation for essential tremor: a systematic review. Mov Disord 2010;25:1550–9.
[8] Marie V, Laurent V, Jean-Luc H, Pierre K, Alim-Louis B, Philippe C, Christelle L. Bilateral deep-brain stimulation of the globus pallidus in primary generalized dystonia. N Engl J Med 2005;9.
[9] Dallapiazza RF, Lee DJ, De Vloo P, Fomenko A, Hamani C, Hodaie M, Kalia SK, Fasano A, Lozano AM. Outcomes from stereotactic surgery for essential tremor. J Neurol Neurosurg Psychiatry 2019;90:474–82.
[10] Coenen VA, Varkuti B, Parpaley Y, Skodda S, Prokop T, Urbach H, Li M, Reinacher PC. Postoperative neuroimaging analysis of DRT deep brain stimulation revision surgery for complicated essential tremor. Acta Neurochir 2017;159:779–87 (Wien).
[11] George MS, Lisanby SH, Sackeim HA. Transcranial magnetic stimulation: applications in neuropsychiatry. Arch Gen Psychiatr 1999;56:300–11.
[12] Olfati N, Shoeibi A, Abdollahian E, Ahmadi H, Hoseini A, Akhlaghi S, Vakili V, Foroughipour M, Rezaeitalab F, Farzadfard M-T, Layegh P, Naseri S. Cerebellar repetitive transcranial magnetic stimulation (rTMS) for essential tremor: a double-blind, sham-controlled, crossover, add-on clinical trial. Brain Stimul 2020;13:190–6.
[13] Shih LC, Pascual-Leone A. Non-invasive brain stimulation for essential tremor. Tremor Hyperkinetic Mov 2017;7:458.
[14] Badran BW, Glusman CE, Austelle CW, Jenkins S, DeVries WH, Galbraith V, Thomas T, Adams TG, George MS, Revuelta GJ. A double-blind, sham-controlled pilot trial of pre-supplementary motor area (Pre-SMA) 1 Hz rTMS to treat essential tremor. Brain Stimul. Basic Transl. Clin. Res. Neuromodulation 2016;9:945–7.
[15] Heller L, van Hulsteyn DB. Brain stimulation using electromagnetic sources: theoretical aspects. Biophys J 1992;63:129–38.
[16] Blackmore J, Shrivastava S, Sallet J, Butler CR, Cleveland RO. Ultrasound neuromodulation: a review of results, mechanisms and safety. Ultrasound Med Biol 2019;45:1509–36.
[17] Ai L, Bansal P, Mueller JK, Legon W. Effects of transcranial focused ultrasound on human primary motor cortex using 7T fMRI: a pilot study. BMC Neurosci 2018;19:56.
[18] Lee C-C, Chou C-C, Hsiao F-J, Chen Y-H, Lin C-F, Chen C-J, Peng S-J, Liu H-L, Yu H-Y. Pilot study of focused ultrasound for drug-resistant epilepsy. Epilepsia 2022;63:162–75.
[19] Maimbourg G, Houdouin A, Deffieux T, Tanter M, Aubry J-F. 3D-printed adaptive acoustic lens as a disruptive technology for transcranial ultrasound therapy using single-element transducers. Phys Med Biol 2018;63:025026.
[20] Marsac L, Chauvet D, La Greca R, Boch A-L, Chaumoitre K, Tanter M, Aubry J-F. Ex vivo optimisation of a heterogeneous speed of sound model of the human skull for non-invasive transcranial focused ultrasound at 1 MHz. Int J Hyperther 2017;33:635–45.
[21] Hynynen K, Sun J. Trans-skull ultrasound therapy: the feasibility of using image-derived skull thickness information to correct the phase distortion. IEEE Trans Ultrason Ferroelectrics Freq Control 1999;46:752–5.
[22] Aubry J-F, Tanter M, Pernot M, Thomas J-L, Fink M. Experimental demonstration of noninvasive transskull adaptive focusing based on prior computed tomography scans. J Acoust Soc Am 2003;113:84–93.
[23] Fry FJ, Ades HW, Fry WJ. Production of reversible changes in the central nervous system by ultrasound. Science 1958;127:83–4.
[24] Boutet A, Ranjan M, Zhong J, Germann J, Xu D, Schwartz ML, Lipsman N, Hynynen K, Devenyi GA, Chakravarty M, Hlasny E, Llinas M, Lozano CS, Elias GJB, Chan J, Coblentz A, Fasano A, Kucharczyk W, Hodaie M, Lozano AM. Focused ultrasound thalamotomy location determines clinical benefits in patients with essential tremor. Brain 2018;141:3405–14.
[25] Li G-F, Zhao H-X, Zhou H, Yan F, Wang J-Y, Xu C-X, Wang C-Z, Niu L-L, Meng L, Wu S, Zhang H-L, Qiu W-B, Zheng H-R. Improved anatomical specificity of non-invasive neuro-stimulation by high frequency (5 MHz) ultrasound. Sci Rep 2016;6:24738.
[26] Increased anatomical specificity of neuromodulation via modulated focused ultrasoundMehić E, Xu JM, Caler CJ, Coulson NK, Moritz CT, Mourad PD, Avenanti A, editors. PLoS One 2014;9:e86939.
[27] Kim H, Park MY, Lee SD, Lee W, Chiu A, Yoo S-S. Suppression of EEG visual-evoked potentials in rats through neuromodulatory focused ultrasound. Neuroreport 2015;26:211–5.
[28] King RL, Brown JR, Pauly KB. Localization of ultrasound-induced in vivo neurostimulation in the mouse model. Ultrasound Med Biol 2014;40:1512–22.
[29] Tufail Y, Matyushov A, Baldwin N, Tauchmann ML, Georges J, Yoshihiro A, Tillery SIH, Tyler WJ. Transcranial pulsed ultrasound stimulates intact brain circuits. Neuron 2010;66:681–94.
[30] He J, Zhu Y, Wu C, Wu J, Chen Y, Yuan M, Cheng Z, Zeng L, Ji X. Simultaneous multi-target ultrasound neuromodulation in freely-moving mice based on a single-element ultrasound transducer. J Neural Eng 2023. https://doi.org/10.1088/1741-2552/acb104.
[31] Ye PP, Brown JR, Pauly KB. Frequency dependence of ultrasound neurostimulation in the mouse brain. Ultrasound Med Biol 2016;42:1512–30.
[32] Yang PS, Kim H, Lee W, Bohlke M, Park S, Maher TJ, Yoo S-S. Transcranial focused ultrasound to the thalamus is associated with reduced extracellular GABA levels in rats. Neuropsychobiology 2012;65:153–60.
[33] Gulick DW, Li T, Kleim JA, Towe BC. Comparison of electrical and ultrasound neurostimulation in rat motor cortex. Ultrasound Med Biol 2017;43:2824–33.
[34] Younan Y, Deffieux T, Larrat B, Fink M, Tanter M, Aubry J-F. Influence of the pressure field distribution in transcranial ultrasonic neurostimulation: influence of pressure distribution in transcranial ultrasonic neurostimulation. Med Phys 2013;40:082902.
[35] Sharabi S, Daniels D, Last D, Guez D, Zivli Z, Castel D, Levy Y, Volovick A, Grinfeld J, Rachmilevich I, Amar T, Mardor Y, Harnof S. Non-thermal focused ultrasound induced reversible reduction of essential tremor in a rat model. Brain Stimul 2019;12:1–8.
[36] Min B-K, Bystritsky A, Jung K-I, Fischer K, Zhang Y, Maeng L-S, In Park S, Chung Y-A, Jolesz FA, Yoo S-S. Focused ultrasound-mediated suppression of chemically-induced acute epileptic EEG activity. BMC Neurosci 2011;12:23.
[37] Zhang J, Zhou H, Yang J, Jia J, Niu L, Sun Z, Shi D, Meng L, Qiu W, Wang X, Zheng H, Wang G. Low-intensity pulsed ultrasound ameliorates depression-like behaviors in a rat model of chronic unpredictable stress. CNS Neurosci Ther 2021;27:233–43.
[38] Yoo S-S, Bystritsky A, Lee J-H, Zhang Y, Fischer K, Min B-K, McDannold NJ, Pascual-Leone A, Jolesz FA. Focused ultrasound modulates region-specific brain activity. Neuroimage 2011;56:1267–75.
[39] Lee W, Lee SD, Park MY, Foley L, Purcell-Estabrook E, Kim H, Fischer K, Maeng L-S, Yoo S-S. Image-guided focused ultrasound-mediated regional brain stimulation in sheep. Ultrasound Med Biol 2016;42:459–70.
[40] Dallapiazza RF, Timbie KF, Holmberg S, Gatesman J, Lopes MB, Price RJ, Miller GW, Elias WJ. Noninvasive neuromodulation and thalamic mapping with low-intensity focused ultrasound. J Neurosurg 2018;128:875–84.
[41] Wattiez N, Constans C, Deffieux T, Tanter M, Aubry J-F, Pouget P. Transcranial ultrasonic stimulation modulates single-neuron discharge in macaques performing an antisaccade task. Brain Stimul 2017:1024–31.
[42] Deffieux T, Younan Y, Wattiez N, Tanter M, Pouget P, Aubry J-F. Low-intensity focused ultrasound modulates monkey visuomotor behavior. Curr Biol 2013;23:2430–3.
[43] Verhagen L, Gallea C, Folloni D, Constans C, Jensen DE, Ahnine H, Roumazeilles L, Santin M, Ahmed B, Lehericy S, Klein-Flügge MC, Krug K, Mars RB, Rushworth MF, Pouget P, Aubry J-F, Sallet J. Offline impact of transcranial focused ultrasound on cortical activation in primates. Elife 2019;8:e40541.
[44] Folloni D, Verhagen L, Mars RB, Fouragnan E, Constans C, Aubry J-F, Rushworth MFS, Sallet J. Manipulation of subcortical and deep cortical activity in the primate brain using transcranial focused ultrasound stimulation. Neuron 2019;101:1109–1116.e5.
[45] Yang P-F, Phipps MA, Jonathan S, Newton AT, Byun N, Gore JC, Grissom WA, Caskey CF, Chen LM. Bidirectional and state-dependent modulation of brain activity by transcranial focused ultrasound in non-human primates. Brain Stimul 2021;14:261–72.
[46] Yang P-F, Phipps MA, Newton AT, Chaplin V, Gore JC, Caskey CF, Chen LM. Neuromodulation of sensory networks in monkey brain by focused ultrasound with MRI guidance and detection. Sci Rep 2018;8:7993.
[47] Dyck PJ, Zimmerman I, Gillen DA, Johnson D, Karnes JL, O'Brien PC. Cool, warm, and heat-pain detection thresholds: testing methods and inferences about anatomic distribution of receptors. Neurology 1993;43:1500. 1500.

[48] Legon W, Sato TF, Opitz A, Mueller J, Barbour A, Williams A, Tyler WJ. Transcranial focused ultrasound modulates the activity of primary somatosensory cortex in humans. Nat Neurosci 2014;17:322–9.

[49] Lee W, Kim H-C, Jung Y, Chung YA, Song I-U, Lee J-H, Yoo S-S. Transcranial focused ultrasound stimulation of human primary visual cortex. Sci Rep 2016;6:34026.

[50] Badran BW, Caulfield KA, Stomberg-Firestein S, Summers PM, Dowdle LT, Savoca M, Li X, Austelle CW, Short EB, Borckardt JJ, Spivak N, Bystritsky A, George MS. Sonication of the anterior thalamus with MRI-Guided transcranial focused ultrasound (tFUS) alters pain thresholds in healthy adults: a double-blind, sham-controlled study. Brain Stimul 2020;13:1805–12.

[51] Krasovitski B, Frenkel V, Shoham S, Kimmel E. Intramembrane cavitation as a unifying mechanism for ultrasound-induced bioeffects. Proc Natl Acad Sci USA 2011;108:3258–63.

[52] Menz MD, Ye P, Firouzi K, Nikoozadeh A, Pauly KB, Khuri-Yakub P, Baccus SA. Radiation force as a physical mechanism for ultrasonic neurostimulation of the *ex vivo* retina. J Neurosci 2019;39:6251–64.

[53] Kim T, Park C, Chhatbar PY, Feld J, Jiang X, Feng W. Effect of low intensity transcranial ultrasound stimulation on neuromodulation in animals and humans: an updated systematic review. Front Neurosci 2021;15. https://doi.org/10.3389/fnins.2021.620863.

[54] King RL, Brown JR, Newsome WT, Pauly KB. Effective parameters for ultrasound-induced in vivo neurostimulation. Ultrasound Med Biol 2013;39:312–31.

[55] Chen H, Felix C, Folloni D, Verhagen L, Sallet J, Jerusalem A. Modelling transcranial ultrasound neuromodulation: an energy-based multiscale framework. Acta Biomater 2022;151:317–32.

[56] Plaksin M, Kimmel E, Shoham S. Cell-type-selective effects of intramembrane cavitation as a unifying theoretical framework for ultrasonic neuromodulation. eneuro 2016;3. ENEURO.0136-15.2016.

[57] Dell'Italia J, Sanguinetti JL, Monti MM, Bystritsky A, Reggente N. Current state of potential mechanisms supporting low intensity focused ultrasound for neuromodulation. Front Hum Neurosci 2022;16. https://doi.org/10.3389/fnhum.2022.872639.

[58] Weinreb E, Moses E. Mechanistic insights into ultrasonic neurostimulation of disconnected neurons using single short pulses. Brain Stimul 2022;15:769–79.

[59] Darrow DP, O'Brien P, Richner TJ, Netoff TI, Ebbini ES. Reversible neuroinhibition by focused ultrasound is mediated by a thermal mechanism. Brain Stimul 2019;12:1439–47.

[60] McIntyre CC, Hahn PJ. Network perspectives on the mechanisms of deep brain stimulation. Neurobiol Dis 2010;38:329–37.

[61] Ashkan K, Rogers P, Bergman H, Ughratdar I. Insights into the mechanisms of deep brain stimulation. Nat Rev Neurol 2017;13:548–54.

[62] Chiken S, Nambu A. Mechanism of deep brain stimulation: inhibition, excitation, or disruption? Neurosci. Rev. J. Bringing Neurobiol. Neurol. Psychiatry 2016;22:313–22.

[63] Khadka N, Harmsen IE, Lozano AM, Bikson M. Bio-Heat model of kilohertz-frequency deep brain stimulation increases brain tissue temperature. Neuromodulation Technol. Neural Interface 2020;23:489–95.

[64] Assistance Publique - Hôpitaux de Paris. *Transcranial ultrasound Therapy of essential tremor* (clinicaltrials.gov. https://clinicaltrials.gov/ct2/show/NCT04074031; 2023.

[65] Fahn S, Tolosa E, Marin C. In: Parkinson's disease and movement disorders. Parkinson's Disease and Movement Disorders; 1988.

[66] Vial F, Kassavetis P, Merchant S, Haubenberger D, Hallett M. How to do an electrophysiological study of tremor. Clin. Neurophysiol. Pract 2019;4:134–42.

[67] Ali SM, Arjunan SP, Peter J, Perju-Dumbrava L, Ding C, Eller M, Raghav S, Kempster P, Motin MA, Radcliffe PJ, Kumar DK. Wearable accelerometer and gyroscope sensors for estimating the severity of essential tremor. IEEE J. Transl. Eng. Health Med. 2024;12:194–203.

[68] van Brummelen EMJ, Ziagkos D, de Boon WMI, Hart EP, Doll RJ, Huttunen T, Kolehmainen P, Groeneveld GJ. Quantification of tremor using consumer product accelerometry is feasible in patients with essential tremor and Parkinson's disease: a comparative study. J. Clin. Mov. Disord. 2020;7:4.

[69] Taren J, Guiot G, Derome P, Trigo JC. Hazards of stereotaxic thalamectomy. J Neurosurg 1968;29:10.

[70] Kwon HG, Hong JH, Hong CP, Lee DH, Ahn SH, Jang SH. Dentatorubrothalamic tract in human brain: diffusion tensor tractography study. Neuroradiology 2011;53:787–91.

[71] Manjón JV, Coupé P. volBrain: an online MRI brain volumetry system. Front Neuroinf 2016;10. https://doi.org/10.3389/fninf.2016.00030.

[72] Lipsman N, Schwartz ML, Huang Y, Lee L, Sankar T, Chapman M, Hynynen K, Lozano AM. MR-guided focused ultrasound thalamotomy for essential tremor: a proof-of-concept study. Lancet Neurol 2013;12:462–8.

[73] Elias WJ, Huss D, Voss T, Loomba J, Khaled M, Zadicario E, Frysinger RC, Sperling SA, Wylie S, Monteith SJ, Druzgal J, Shah BB, Harrison M, Wintermark M. A pilot study of focused ultrasound thalamotomy for essential tremor. N Engl J Med 2013;369:640–8.

[74] Inc. Insightec, exablate 4000 type 1.1 SW 7.2 operator manual CE Rev5, vol. 8; 2019.

[75] Bancel T, Houdouin A, Annic P, Rachmilevitch I, Shapira Y, Tanter M, Aubry J-F. Comparison between ray-tracing and full-wave simulation for transcranial ultrasound focusing on a clinical system using the transfer matrix formalism. IEEE Trans Ultrason Ferroelectrics Freq Control 2021;68:2554–65.

[76] Gallay MN, Moser D, Jeanmonod D. Safety and accuracy of incisionless transcranial MR-guided focused ultrasound functional neurosurgery: single-center experience with 253 targets in 180 treatments. J Neurosurg 2018;130:1234–43.

[77] Pineda-Pardo JA, Martínez-Fernández R, Rodríguez-Rojas R, Del-Alamo M, Hernández F, Foffani G, Dileone M, Máñez-Miró JU, De Luis-Pastor E, Vela L, Obeso JA. Microstructural changes of the dentato-rubro-thalamic tract after transcranial MR guided focused ultrasound ablation of the posteroventral VIM in essential tremor. Hum Brain Mapp 2019;40:2933–42.

[78] Chang WS, Jung HH, Kweon EJ, Zadicario E, Rachmilevitch I, Chang JW. Unilateral magnetic resonance guided focused ultrasound thalamotomy for essential tremor: practices and clinicoradiological outcomes. J Neurol Neurosurg Psychiatry 2014;86:257–64.

[79] Pouget P, Frey S, Ahnine H, Attali D, Claron J, Constans C, Aubry J-F, Arcizet F. Neuronavigated repetitive transcranial ultrasound stimulation induces long-lasting and reversible effects on oculomotor performance in non-human primates. Front Physiol 2020;11:1042.

[80] Rieke V, Butts Pauly K. MR thermometry. J Magn Reson Imag 2008;27:376–90.

[81] Zeng K, Darmani G, Fomenko A, Xia X, Tran S, Nankoo J-F, Shamli Oghli Y, Wang Y, Lozano AM, Chen R. Induction of human motor cortex plasticity by theta burst transcranial ultrasound stimulation. Ann Neurol 2022;91:238–52.

[82] Zhang Y, Ren L, Liu K, Tong S, Yuan T-F, Sun J. Transcranial ultrasound stimulation of the human motor cortex. iScience 2021;24:103429.

[83] Systematic examination of low-intensity ultrasound parameters on human motor cortex excitability and behaviorFomenko A, Chen K-HS, Nankoo J-F, Saravanamuttu J, Wang Y, El-Baba M, Xia X, Seerala SS, Hynynen K, Lozano AM, Chen R, Ivry RB, Dugué L, Legon W, editors. Elife 2020;9:e54497.

[84] Legon W, Bansal P, Tyshynsky R, Ai L, Mueller JK. Transcranial focused ultrasound neuromodulation of the human primary motor cortex. Sci Rep 2018;8:10007.

[85] Zeng K, Li Z, Xia X, Wang Z, Darmani G, Li X, Chen R. Effects of different sonication parameters of theta burst transcranial ultrasound stimulation on human motor cortex. Brain Stimul 2024;17:258–68.

[86] Shamli Oghli Y, Grippe T, Arora T, Hoque T, Darmani G, Chen R. Mechanisms of theta burst transcranial ultrasound induced plasticity in the human motor cortex. Brain Stimul 2023;16:1135–43.

[87] Bao S, Kim H, Shettigar NB, Li Y, Lei Y. Personalized depth-specific neuromodulation of the human primary motor cortex via ultrasound. J Physiol 2024;602:933–48.

[88] Zhang T, Guo B, Zuo Z, Long X, Hu S, Li S, Su X, Wang Y, Liu C. Excitatory-inhibitory modulation of transcranial focus ultrasound stimulation on human motor cortex. CNS Neurosci Ther 2023;29:3829–41.

[89] Nakajima K, Osada T, Ogawa A, Tanaka M, Oka S, Kamagata K, Aoki S, Oshima Y, Tanaka S, Konishi S. A causal role of anterior prefrontal-putamen circuit for response inhibition revealed by transcranial ultrasound stimulation in humans. Cell Rep 2022;40:111197.

[90] Samuel N, Ding MYR, Sarica C, Darmani G, Harmsen IE, Grippe T, Chen X, Yang A, Nasrkhani N, Zeng K, Chen R, Lozano AM. Accelerated transcranial ultrasound neuromodulation in Parkinson's disease: a pilot study. Mov Disord 2023;38:2209–16.

[91] Pinton G, Aubry J-F, Bossy E, Muller M, Pernot M, Tanter M. Attenuation, scattering, and absorption of ultrasound in the skull bone: absorption of ultrasound in the skull bone. Med Phys 2011;39:299–307.

[92] Constans C, Mateo P, Tanter M, Aubry J-F. Potential impact of thermal effects during ultrasonic neurostimulation: retrospective numerical estimation of temperature elevation in seven rodent setups. Phys Med Biol 2018;63:025003.

[93] Duck FA. Medical and non-medical protection standards for ultrasound and infrasound. Prog Biophys Mol Biol 2007;93:176–91.

[94] Blomqvist A, Zhang E-T, Craig AD. Cytoarchitectonic and immunohistochemical characterization of a specific pain and temperature relay, the posterior portion of the ventral medial nucleus, in the human thalamus. Brain 2000;123:601–19.

[95] Coenen VA, Sajonz B, Prokop T, Reisert M, Piroth T, Urbach H, Jenkner C, Reinacher PC. The dentato-rubro-thalamic tract as the potential common deep brain stimulation target for tremor of various origin: an observational case series. Acta Neurochir (Wien) 2020;162:1053–66.

[96] Kremer NI, Pauwels RWJ, Pozzi NG, Lange F, Roothans J, Volkmann J, Reich MM. Deep brain stimulation for tremor: update on long-term outcomes, target considerations and future directions. J Clin Med 2021;10:3468.

[97] Dembek TA, Petry-Schmelzer JN, Reker P, Wirths J, Hamacher S, Steffen J, Dafsari HS, Hövels M, Fink GR, Visser-Vandewalle V, Barbe MT. PSA and VIM DBS efficiency in essential tremor depends on distance to the dentatorubrothalamic tract. NeuroImage Clin 2020;26:102235.

[98] Marsac L, Chauvet D, Larrat B, Pernot M, Robert B, Fink M, Boch AL, Aubry JF, Tanter M. MR-guided adaptive focusing of therapeutic ultrasound beams in the human head: MR-guided adaptive focusing of therapeutic ultrasound beams. Med Phys 2012;39:1141–9.

[99] Sanguinetti JL, Hameroff S, Smith EE, Sato T, Daft CMW, Tyler WJ, Allen JJB. Transcranial focused ultrasound to the right prefrontal cortex improves mood and alters functional connectivity in humans. Front Hum Neurosci 2020;14:52.

[100] Reznik SJ, Sanguinetti JL, Tyler WJ, Daft C, Allen JJB. A double-blind pilot study of transcranial ultrasound (TUS) as a five-day intervention: TUS mitigates worry among depressed participants. Neurol Psychiatr Brain Res 2020;37:60–6.
[101] Zhuang X, He J, Wu J, Ji X, Chen Y, Yuan M, Zeng L. A spatial multi-target ultrasound neuromodulation system using high-powered 2-D array transducer. IEEE Trans Ultrason Ferroelectrics Freq Control 2022:1. 1.
[102] Constans C, Deffieux T, Pouget P, Tanter M, Aubry J-F. A 200–1380-kHz quadrifrequency focused ultrasound transducer for neurostimulation in rodents and primates: transcranial in vitro calibration and numerical study of the influence of skull cavity. IEEE Trans Ultrason Ferroelectrics Freq Control 2017;64:717–24.
[103] Kamimura HAS, Wang S, Chen H, Wang Q, Aurup C, Acosta C, Carneiro AAO, Konofagou EE. Focused ultrasound neuromodulation of cortical and subcortical brain structures using 1.9 MHz. Med Phys 2016;43:5730–5.